

TECHNICAL REPORT STANDARD TITLE PAGE

1. REPORT NO. WA-RD 452.1	2. GOVERNMENT ACCESSION NO.	3. RECIPIENT'S CATALOG NO.	
4. TITLE AND SUBTITLE Geosynthetic Reinforced Wall Analysis Phase II: Use of In-Soil Geosynthetic Behavior to Predict Deformations Volume 1: Research Program and Results		5. REPORT DATE August 1998	
		6. PERFORMING ORGANIZATION CODE	
7. AUTHOR(S) Robert D. Holtz and Wei F. Lee		8. PERFORMING ORGANIZATION REPORT NO.	
9. PERFORMING ORGANIZATION NAME AND ADDRESS Washington State Transportation Center (TRAC) University of Washington, Box 354802 University District Building; 1107 NE 45th Street, Suite 535 Seattle, Washington 98105-4631		10. WORK UNIT NO.	
		11. CONTRACT OR GRANT NO. Contract T9903, Task 33	
12. SPONSORING AGENCY NAME AND ADDRESS Washington State Department of Transportation Transportation Building, MS 7370 Olympia, Washington 98504-7370		13. TYPE OF REPORT AND PERIOD COVERED Research Report	
		14. SPONSORING AGENCY CODE	
15. SUPPLEMENTARY NOTES This study was conducted in cooperation with the U.S. Department of Transportation, Federal Highway Administration.			
16. ABSTRACT <p>As part of the reconstruction of Interstate 90 in Seattle, Washington, WSDOT designed and supervised the construction of a geosynthetic reinforced soil (GRS) retaining wall located on Rainier Avenue, Seattle. The Rainier Avenue wall had a maximum height of 12.6 m and supported a nearly 6-m-high surcharge fill. At the time it was constructed, it was the highest GRS wall in the world. The wall was extensively instrumented and monitored during and after construction to evaluate its face deflections and the strain levels occurring in it.</p> <p>To define the actual stress distribution occurring in the Rainier Avenue wall, a two-phase research project was conducted by the University of Washington. Phase I included an extensive laboratory test program that used a newly developed plane strain device. Numerical analysis and modeling of the results of the instrumentation and laboratory tests constituted Phase II.</p> <p>The major tasks of the Phase II project were to (1) analyze the test result of the unit cell device (UCD), a plane strain GRS element testing device developed in Phase I; (2) develop numerical models of the Rainier Avenue Wall using both material properties and test results of the UCD; and (3) using the results of tasks 1 and 2, develop a methodology for analyzing the working stress-strain distribution in the GRS retaining structures.</p> <p>The Phase II project was conducted from September 1995 to December 1997. During this period, two research programs were conducted simultaneously. One program concentrated on analyzing the UCD test results, and the other on developing the numerical models of the Rainier Avenue wall. Significant results were obtained from both research programs. Products of the Phase II research include an elasticity model that is capable of analyzing GRS behavior, composite properties of GRS elements, and four numerical models of the Rainier Avenue wall. Improved understanding of the working stress-strain distribution inside GRS retaining structures was also obtained with these products.</p>			
17. KEY WORDS geosynthetic reinforced soil, retaining wall		18. DISTRIBUTION STATEMENT No restrictions. This document is available to the public through the National Technical Information Service, Springfield, VA 22616	
19. SECURITY CLASSIF. (of this report) None	20. SECURITY CLASSIF. (of this page) None	21. NO. OF PAGES 32	22. PRICE

Research Report,
Research Project T9903, Task 33
Geo Reinforcement II

**GEOSYNTHETIC REINFORCED WALL ANALYSIS
PHASE II: USE OF IN-SOIL GEOSYNTHETIC
BEHAVIOR TO PREDICT DEFORMATIONS**

Volume 1: Research Program and Results

by

Robert D. Holtz
Professor

Wei F. Lee
Research Assistant

Department of Civil Engineering
University of Washington, Box 352700
Seattle, Washington 98195-2700

Washington State Transportation Center (TRAC)
University of Washington, Box 354802
University District Building
1107 NE 45th Street, Suite 535
Seattle, Washington 98105-4631

Washington State Department of Transportation
Technical Monitor
Tony Allen
State Geotechnical Engineer

Prepared for

Washington State Transportation Commission
Department of Transportation
and in cooperation with
U.S. Department of Transportation
Federal Highway Administration

August 1998

DISCLAIMER

The contents of this report reflect the views of the authors, who are responsible for the facts and the accuracy of the data presented herein. The contents do not necessarily reflect the official views or policies of the Washington State Transportation Commission, Department of Transportation, or the Federal Highway Administration. This report does not constitute a standard, specification, or regulation.

TABLE OF CONTENTS

<u>Section</u>	<u>Page</u>
1. Introduction	1
1.1. Background	1
1.2. Scope of Phase II Project	1
2. Phase II Research Program	3
2.1. Analysis of Unit Cell Device Test Results	3
2.2. Numerical Geosynthetic Reinforced Retaining Structure Models	3
2.2.1. Complex Models	4
2.2.2. Composite Property Models	4
3. Results and Discussion	5
3.1. Behavior of Geosynthetic Reinforced Soil Element	5
3.1.1. Transversely Isotropic Elasticity Model for a GRS Element with Plane Strain Loading Conditions	5
3.1.2. Interpreting UCD Test Results Using Transversely Isotropic Elasticity Model	7
3.1.3. Composite GRS Moduli	8
3.2. Numerical Models	14
3.2.1. Models 5008 and 5008p2	15
3.2.2. Models COMPA and COMPS	24
4. Conclusions and Suggestions	29
5. References	31
6. Bibliography	32

LIST OF FIGURES

<u>Figure</u>		<u>Page</u>
1.	Geosynthetic Reinforced Soil Element	4
2.	Plane Strain Soil Moduli Obtained from UCD Tests	11
3.	Horizontal Composite Moduli of GRS at 1% Horizontal Strain and with $v_{hh}=0.3$	12
4.	Vertical Composite Moduli of GRS at 1% Horizontal Strain and with $v_{hh}=0.3$	12
5.	Face Deflection Results of Models 5008 and 5008p2.	18
6.	Inclinometer Deflection Results of Models 5008 and 5008p2	19
7.	Strain Distribution along the Instrumented Layers, after Wall Construction	20
8.	Strain Distribution along the Instrumented Layers, after Surcharge	21
9.	Maximum Deflection versus Geosynthetic Modulus	22
10.	Maximum Deflection versus Soil Friction Angle	23
11.	Maximum Deflection versus Soil Cohesion	23
12.	Maximum Deflection versus Soil Moduli	24
13.	Face Deflection Result of Model COMPA	26
14.	Inclinometer Deflection Result of Model COMPA	26
15.	Face Deflection Result of Model COMPS	27
16.	Inclinometer Deflection Result of Model COMPS	27

LIST OF TABLES

<u>Table</u>		<u>Page</u>
1.	General Information of UCD Tests	9
2.	Sampled Stress-Strain Information from UCD Tests	10
3.	Coefficients A, B, C, and D for Equations (10) and (11), for 1% Horizontal Strain and Poisson's Ratio 0.3	13

1. INTRODUCTION

1.1. BACKGROUND

As part of the reconstruction of Interstate 90 in Seattle, Washington, WSDOT designed and supervised the construction of a geosynthetic reinforced soil (GRS) retaining wall located on Rainier Avenue, Seattle. The Rainier Avenue wall had a maximum height of 12.6 m and supported a nearly 6-m-high surcharge fill. At the time it was constructed, it was the highest GRS wall in the world (Allen et al., 1992). The wall was extensively instrumented and monitored during and after construction to evaluate its face deflections and the strain levels occurring in it (Christopher, et al., 1990). Results of the instrumentation have been reported by Holtz et al. (1991) and Allen et al. (1992).

To define the actual stress distribution occurring in the Rainier Avenue wall, a two-phase research project was conducted by the University of Washington. Phase I included an extensive laboratory test program that used a newly developed plane strain device. Numerical analysis and modeling of the results of the instrumentation and laboratory tests constituted Phase II.

1.2. SCOPE OF PHASE II PROJECT

The major tasks of the Phase II project were to

1. analyze the test result of the unit cell device (UCD), a plane strain GRS element testing device developed in Phase I
2. develop numerical models of the Rainier Avenue Wall using both material properties and test results of the UCD
3. using the results of tasks 1 and 2, develop a methodology for analyzing the working stress-strain distribution in the GRS retaining structures.

The Phase II project was conducted from September 1995 to December 1997. During this period, two research programs were conducted simultaneously. One program

concentrated on analyzing the UCD test results, and the other on developing the numerical models of the Rainier Avenue wall. Significant results were obtained from both research programs. Products of the Phase II research include an elasticity model that is capable of analyzing GRS behavior, composite properties of GRS elements, and four numerical models of the Rainier Avenue wall. Improved understanding of the working stress-strain distribution inside GRS retaining structures was also obtained with these products.

This report consists of three parts:

1. description of the Phase II research program
2. results of the Phase II research
3. conclusions of Phase II research and suggestions for future research.

2. PHASE II RESEARCH PROGRAM

2.1. ANALYSIS OF UNIT CELL DEVICE TEST RESULTS

The UCD was designed and fabricated in Phase I to simulate a GRS element inside GRS retaining structures. It is a load controlled device that tests GRS elements under plane strain conditions (the stress conditions inside a soil retaining structure). Both in-soil properties of geosynthetics and GRS composite properties are measured in the device.

A GRS element inside a reinforced soil structure has different directional stress-strain behaviors because of the reinforcement (Fig. 1). Therefore, instead of an isotropic elasticity approach, anisotropic elasticity was used to interpret the UCD test results correctly. The process for analyzing the behavior of a GRS element, i.e., interpreting the UCD test results correctly, followed the steps listed below:

1. develop an anisotropic elasticity model for GRS composite elements under plane strain loading conditions
2. introduce UCD test results into the developed anisotropic elasticity model to solve for the composite properties of GRS elements
3. develop a methodology for utilizing the composite GRS properties in the GRS retaining structures modeling.

The results of this part of the research are described in section 3 of this report.

2.2. NUMERICAL GRS RETAINING STRUCTURE MODELS

An important task in Phase II was to develop numerical models of the Rainier Avenue wall. The developed numerical models had to be capable of reproducing the instrumentation measurements from the Rainier Avenue wall and of providing information about the stress and strain occurring inside the wall. Two types of models were developed, complex models and composite property models.

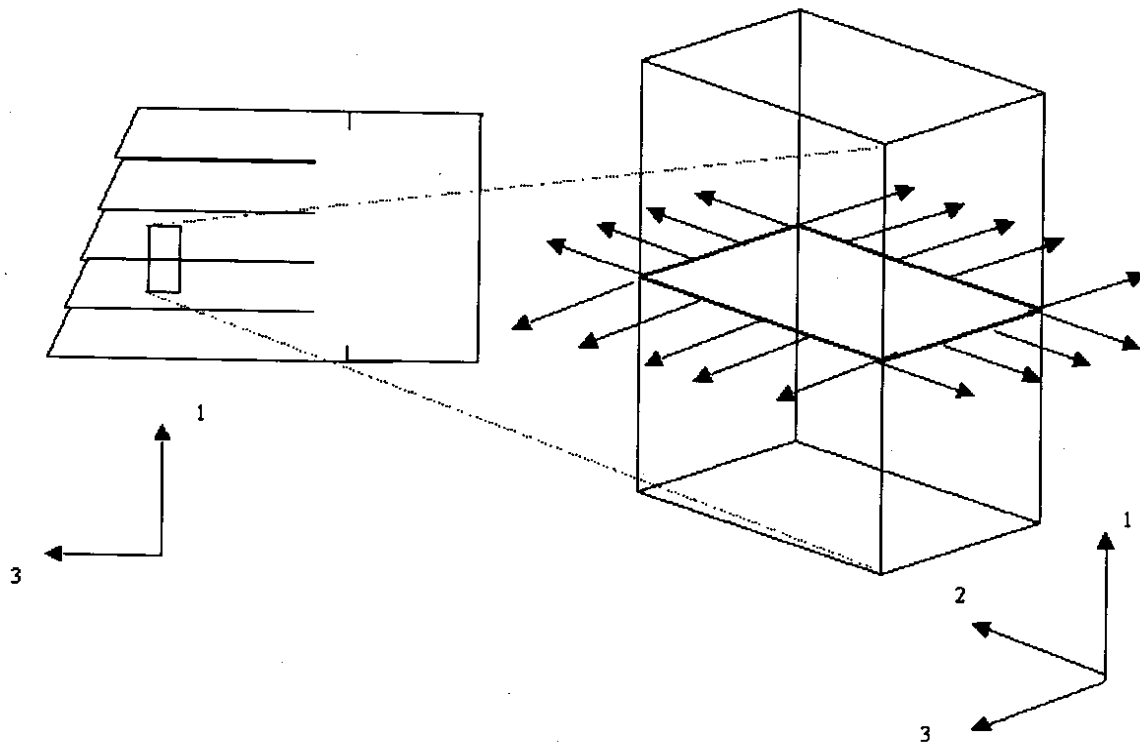


Figure 1. Geosynthetic Reinforced Soil Element.

2.2.1. Complex Models

In complex models, both the geosynthetic reinforcement and the soil are modeled with separate soil and geosynthetics elements. The material properties of the soil and geosynthetics are used as the input to these models. The models should simulate the wall performance after construction and after surcharge load has been applied.

2.2.2. Composite Property Models

In composite property models, GRS elements are modeled as homogeneous composite elements. Only GRS composite elements exist in the composite properties model; i.e. there are no separate soil and geosynthetics elements. The GRS composite properties obtained from UCD test analysis were the input for these models.

3. RESULTS AND DISCUSSION

3.1. BEHAVIOR OF GEOSYNTHETIC REINFORCED SOIL ELEMENT

3.1.1 Transversely Isotropic Elasticity Model for a GRS Element with Plane Strain Loading Conditions

Similar to a UCD test specimen, a GRS element contains different reinforcing mechanisms in different principal directions. For the element shown in Fig. 1, in the horizontal directions, soil is reinforced by the tensile force developed along the geosynthetic and then transmitted into the soil. In the vertical direction, soil is also reinforced because additional resistance to the gravity force is provided by the horizontally placed reinforcement. Therefore, a composite material and anisotropy elasticity approach was applied to characterize the different stress-strain behaviors in the different principal directions inside a GRS element.

In Fig. 1, the vertical direction is defined as direction 1, and the horizontal directions are defined as directions 2 and 3. The geosynthetic reinforcement was placed on a plane perpendicular to direction 1 but also parallel to directions 2 and 3. Thus, the different reinforcing mechanisms of a GRS element in different principal directions were described using orthotropic anisotropic elasticity (Eq.1).

$$\begin{bmatrix} \epsilon_{11} \\ \epsilon_{22} \\ \epsilon_{33} \\ \gamma_{12} \\ \gamma_{23} \\ \gamma_{31} \end{bmatrix} = \begin{bmatrix} \frac{1}{E_1} & -\nu_{21} & -\nu_{31} & 0 & 0 & 0 \\ -\nu_{12} & \frac{1}{E_2} & -\nu_{32} & 0 & 0 & 0 \\ -\nu_{13} & -\nu_{23} & \frac{1}{E_3} & 0 & 0 & 0 \\ 0 & 0 & 0 & \frac{1}{\mu_{12}} & 0 & 0 \\ 0 & 0 & 0 & 0 & \frac{1}{\mu_{23}} & 0 \\ 0 & 0 & 0 & 0 & 0 & \frac{1}{\mu_{31}} \end{bmatrix} \times \begin{bmatrix} \sigma_{11} \\ \sigma_{22} \\ \sigma_{33} \\ \tau_{12} \\ \tau_{23} \\ \tau_{31} \end{bmatrix} \quad (1)$$

In Eq.1, E_1 , E_2 , E_3 , ν_{32} , ν_{23} , ν_{13} , ν_{12} , ν_{21} , and ν_{31} are defined as the composite moduli and Poisson's ratios of the GRS element.

To obtain the composite moduli of the GRS element, only Eq.2, the normal part of Eq.1, needs to be solved. In Eq.2, directions 2 and 3 have different stress-strain composite properties when the mechanical properties of the geosynthetics in the machine direction are different from their properties in the cross-machine direction. However, to further simplify the problem, we assume that the geosynthetic has the same in-soil stress-strain strength properties in both the machine and cross-machine directions. Given this assumption, the same stress-strain behavior is assigned to directions 2 and 3. Eq.2, from orthotropic elasticity, can then be simplified to transversely isotropic elasticity, Eq.3, by using the relations: $E_1 = E_v$, $E_2 = E_3 = E_h$, $\nu_{32} = \nu_{23} = \nu_{hh}$, $\nu_{31} = \nu_{21} = \nu_{hv}$, and $\nu_{13} = \nu_{12} = \nu_{vh}$. For the stress-strain behavior of a GRS element inside soil structures like retaining walls, long embankments, or slopes, plane strain loading conditions are appropriate. Plane strain conditions indicate that there is no strain in direction 2 (i.e. $\epsilon_{22} = \gamma_{12} = \gamma_{23} = 0$). Equations 4 and 5 are expanded from Eq.3 with plane strain loading conditions applied. These two

$$\begin{bmatrix} \epsilon_{11} \\ \epsilon_{22} \\ \epsilon_{33} \end{bmatrix} = \begin{bmatrix} \frac{1}{E_1} & -\frac{\nu_{21}}{E_2} & -\frac{\nu_{31}}{E_3} \\ -\frac{\nu_{21}}{E_1} & \frac{1}{E_2} & -\frac{\nu_{32}}{E_3} \\ -\frac{\nu_{31}}{E_1} & -\frac{\nu_{23}}{E_2} & \frac{1}{E_3} \end{bmatrix} \begin{bmatrix} \sigma_{11} \\ \sigma_{22} \\ \sigma_{33} \end{bmatrix} \quad (2)$$

$$\begin{bmatrix} \epsilon_{11} \\ \epsilon_{22} \\ \epsilon_{33} \end{bmatrix} = \begin{bmatrix} \frac{1}{E_v} & -\frac{\nu_{hv}}{E_h} & -\frac{\nu_{hv}}{E_h} \\ -\frac{\nu_{vh}}{E_v} & \frac{1}{E_h} & -\frac{\nu_{hh}}{E_h} \\ -\frac{\nu_{vh}}{E_v} & -\frac{\nu_{hh}}{E_h} & \frac{1}{E_h} \end{bmatrix} \begin{bmatrix} \sigma_{11} \\ \sigma_{22} \\ \sigma_{33} \end{bmatrix} \quad (3)$$

$$\epsilon_{22} = 0 = -\nu_{vh} \frac{\sigma_{11}}{E_v} + \frac{\sigma_{22}}{E_h} - \nu_{hh} \frac{\sigma_{33}}{E_h} \quad (4)$$

$$\begin{bmatrix} \epsilon_{11} \\ \epsilon_{33} \end{bmatrix} = \begin{bmatrix} \left(\frac{1}{E_v} - \frac{\nu_{hv}^2}{E_h} \right) & \left(\frac{-\nu_{hv} - \nu_{hv}\nu_{hh}}{E_h} \right) \\ \left(\frac{-\nu_{hv} - \nu_{hv}\nu_{hh}}{E_h} \right) & \left(\frac{1}{E_h} - \frac{\nu_{hh}^2}{E_h} \right) \end{bmatrix} \begin{bmatrix} \sigma_{11} \\ \sigma_{33} \end{bmatrix} \quad (5)$$

equations therefore represent the transversely isotropic elasticity model for a GRS element under plane strain loading conditions. Composite moduli of the GRS element can be solved with this model with adequate material testing data, e.g., from the UCD test results.

3.1.2 Interpreting UCD Test Results Using the Transversely Isotropic Elasticity Model

The UCD was designed to test a GRS element under plane strain loading conditions to simulate the GRS element inside GRS soil structures. The UCD specimen is exactly like the GRS element shown in Fig. 1 with plane strain loading conditions. Therefore, the developed transversely isotropic elasticity model could be applied to interpret the UCD test results. Equations 6 to 8 are rearranged from Eqs. 4 and 5. Terms σ_{11} , σ_{22} , σ_{33} , ϵ_{11} , and ϵ_{33} in Eqs. 6 to 8 were obtained by reducing the UCD test data. However, there were still four unknowns (E_v , E_h , ν_{hh} , and ν_{hv}) remaining in Eqs. 6 to 8. Numerical analysis was performed to solve Eqs. 6 to 8. The steps of the numerical analysis were as follows:

1. Formulating a spreadsheet using Eqs. 6 to 8,

$$\nu_{hv} = \frac{\sigma_{22} - \nu_{hh}\sigma_{33}}{\sigma_{11}} \quad (6)$$

$$E_h = \frac{1}{\epsilon_{33}} \cdot [B\sigma_{11} + (1-C)\sigma_{33}] \quad (7)$$

$$E_v = \frac{E_h \cdot \sigma_{11}}{\epsilon_{11} E_h + A \sigma_{11} - B \sigma_{33}} \quad (8)$$

where $A = \nu_{hv}^2$

$$B = -\nu_{hv} - \nu_{hv} \nu_{hh}$$

$$C = \nu_{hh}^2$$

$$\text{Also } \nu_{vh} = \nu_{hv} E_v / E_h$$

2. Inserting a reasonable range of values for Poisson's ratios ν_{hh} into the spreadsheet
3. Computing the composite moduli E_v and E_h using the spreadsheet.

3.1.3 Composite GRS Moduli

UCD test data were input into the developed transversely isotropic elasticity model to solve for the composite GRS moduli. Table 1 shows the test numbers, effective soil confining pressures, and geosynthetics information for the UCD tests that were used to solve the composite moduli. Table 2 shows the sampled stress and strain information that was reduced from the raw UCD test data. The stress and strain information was sampled at conditions when the lateral strain equaled 1 percent and for a horizontal plane Poisson's ratio equal to 0.3.

To observe the reinforcing effect in both the vertical and horizontal directions, the transversely isotropic elasticity model was also applied to soil-only UCD tests to obtain the plane strain vertical and horizontal soil moduli. Figure 2 shows the plane strain soil moduli results. Larger moduli were found in the horizontal direction than in vertical direction because the UCD specimens were compacted to the desired density during specimen preparation. Both horizontal and vertical plane strain moduli increased as effective soil confining pressure increased. The horizontal plane strain moduli increased linearly as effective soil confining pressure increased; however, the vertical plane strain moduli increase was less at higher effective soil confining pressures.

Table 1. General Information of UCD Tests

UCD Test No. (Boyle, 1995)	Effective Soil Confining Pressure (kPa)	Geosynthetic Information (Name, 2% Mwwt ¹ (kN/m), material type)
115	12.4	Soil only
79	12.3	GTF 200, 103, polypropylene
77	10.4	GTF 375, 204, polypropylene
76	11.2	GTF 500, 357, polypropylene
98	10.6	GTF 1225T, 1126, polyester
112	24.6	Soil only
65	23.9	GTF 200, 103, polypropylene
67	23.3	GTF 200, 103, polypropylene
74	23.5	GTF 200, 103, polypropylene
81	23.1	GTF 200, 103, polypropylene
70	21.7	GTF 375, 204, polypropylene
73	22.0	GTF 375, 204, polypropylene
71	19.3	GTF 500, 357, polypropylene
99	22.5	GTF 1225T, 1126, polyester
100	25.0	GTF 1225T, 1126, polyester
111	21.3	GTF 1225T, 1126, polyester
54	47.6	Soil only
62	47.5	GTF 200, 103, polypropylene
55	43.6	GTF 375, 204, polypropylene
106	47.3	GTF 1225T, 1126, polyester

¹ Mwwt: Wide Width Tensile Test Modulus (ASTM D 4595)

Table 2. Sampled Stress-Strain Information from UCD tests

UCD Test No. (Boyle, 1995)	Vertical Strain (%)	Horizontal Strain (%)	Vertical Stress (kPa)	Lateral Stress ² (kPa)	Effective Reinforced Lateral Stress ³ (kPa)
115	0.63	0.52	88.6	80.2	12.4
79	0.92	1.04	248.5	241.8	20.7
77	1.28	1.00	312.9	303.9	26.4
76	1.42	1.00	376.4	368.3	32.0
98	1.26	1.00	498.5	489.4	61.5
112	0.49	1.00	217.8	197.9	24.6
65	1.09	1.00	345.9	326.1	32.9
67	1.12	1.00	344.0	327.7	28.3
74	1.17	1.01	351.9	330.8	30.2
81	1.13	1.01	319.9	299.7	28.4
70	1.19	1.00	396.1	376.7	37.9
73	1.45	1.01	413.5	392.7	37.1
71	1.49	1.00	531.6	512.4	47.1
99	1.36	1.00	593.8	574.3	76.1
100	1.36	1.00	522.5	503.0	64.6
111	1.78	1.00	765.0	745.6	90.7
54	0.83	1.01	306.8	263.4	47.6
62	1.21	1.00	423.9	379.9	54.5
55	0.98	1.00	514.2	470.8	55.8
106	1.45	1.00	835.6	791.1	98.7

² Lateral stress in the direction which there is no strain (plane strain controlled direction).

³ Calculated using equation $\sigma_{3E} = \sigma_{3C} + \frac{T_{in-soil}}{A}$ (Boyle, 1995), A = effective lateral area of specimen.

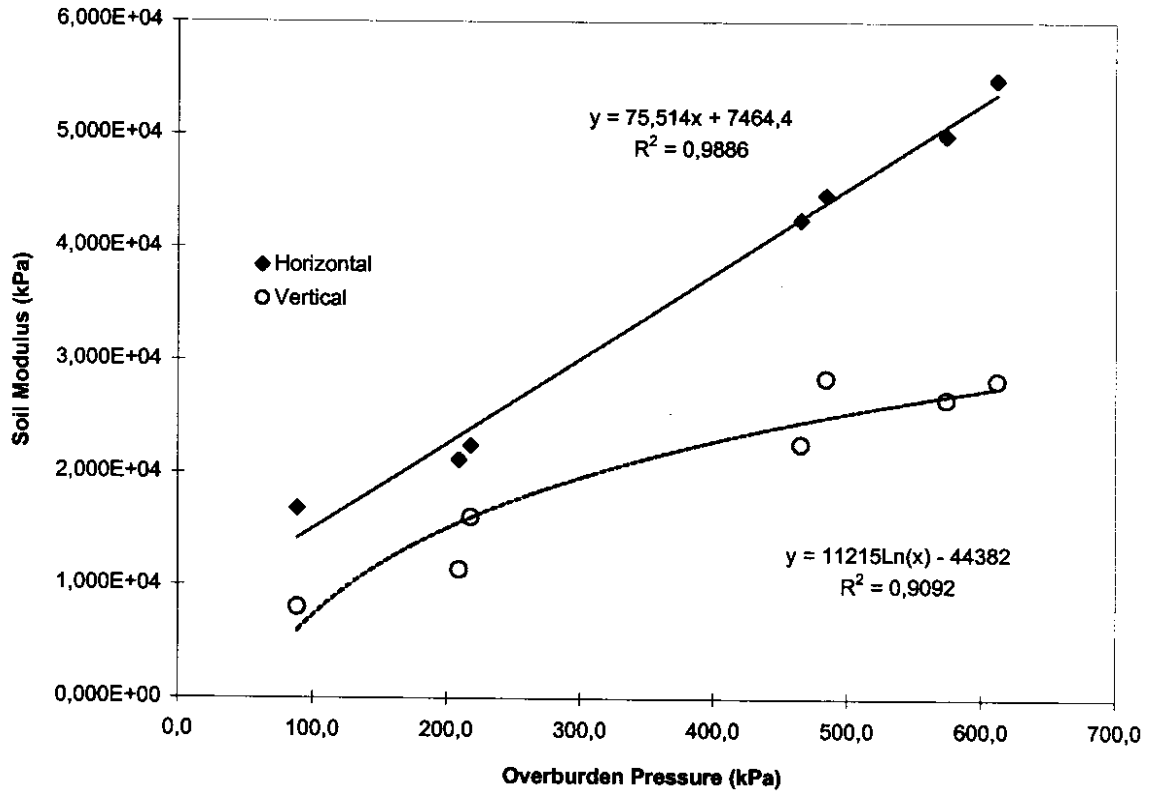


Figure 2. Plane Strain Soil Moduli Obtained from UCD tests.

Figure 3 shows the results of horizontal GRS composite moduli versus the effective soil confining pressure (ESCP), and Fig. 4 shows the results of vertical GRS composite moduli versus the ESCP. ESCP is the confining pressure that is contributed by soil only, without the confining pressure that is contributed by the tensile strength of geosynthetic reinforcement. ESCP can be estimated with an empirical equation:

$$\sigma_{\text{ESCP}} = K_s \cdot \sigma_{\text{ov}} \quad (9)$$

where σ_{ESCP} = Effective Soil Confining Pressure

K_s = Effective Lateral Earth Pressure Ratio

σ_{ov} = Overburden Pressure

As shown in Figs. 3 and 4, both vertical and horizontal composite moduli of GRS increase as the effective soil confining pressure increases for single geosynthetic reinforcement. For

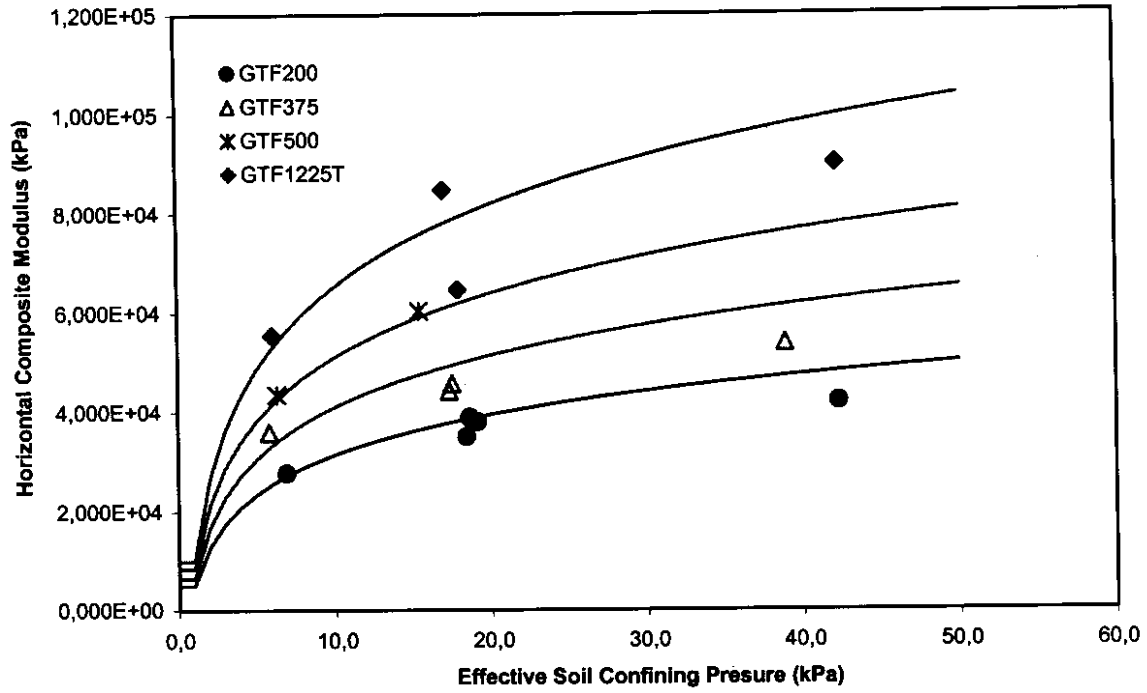


Figure 3. Horizontal Composite Moduli of GRS at 1% Horizontal Strain and with $\nu_{hh}=0.3$.

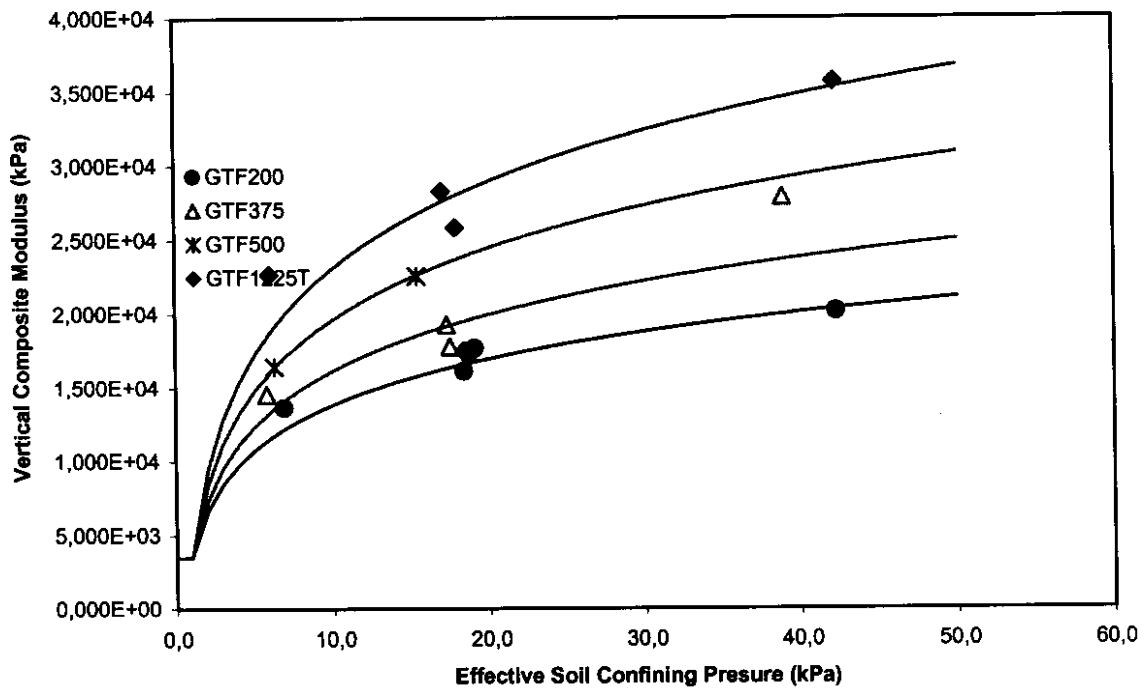


Figure 4. Vertical Composite Moduli of GRS at 1% Horizontal Strain and with $\nu_{hh}=0.3$.

different geosynthetic reinforcements, the tendency was also observed that composite moduli increase as in-isolation tensile moduli of geosynthetic reinforcements increase. In both the horizontal and vertical directions, GRS composite moduli were found to be larger than the plane strain soil moduli. This proves that the geosynthetics contribute to the reinforcing function in the horizontal as well as in the vertical direction. Moreover, all the horizontal GRS composite moduli were found to be larger than all the vertical GRS composite moduli for GRS reinforced soil for certain geosynthetics under the ESCP range tested by Boyle (1995). This result confirms that the horizontal direction is the major reinforcing direction.

Empirical equations (Eqs. 10 and 11) were also developed in an effort to characterize the moduli numerically (as the solid lines shown in Figs. 3 and 4).

$$M_{HC} = A \cdot \log \sigma_{ESCP} + B \quad (10)$$

$$M_{VC} = C \cdot \log \sigma_{ESCP} + D \quad (11)$$

where M_{HC} = horizontal GRS composite modulus, in kPa

M_{VC} = vertical GRS composite modulus, in kPa

A, B, C, D, are coefficients determined from UCD test data (Table 3).

Table 3. Coefficient A, B, C, and D for Equation (10) and (11), for 1% Horizontal Strain and Poisson's Ratio 0.3

Geosynthetics	A	B	C	D
GTF 200	10500	4000	4500	2500
GTF 375	12500	6000	5000	3000
GTF 500	16500	8000	6000	3500
GTF 1225t	22500	9000	8000	3700

3.2 NUMERICAL MODELS

Two kinds of numerical models were developed in this research project in an attempt to reproduce the Rainier Avenue wall field instrumentation measurements. Both models were developed with a commercial finite difference computer program: FLAC (Fast Lagrangian Analysis of Continua). Models 5008 and 5008p2 were the complex models that simulated the Rainier Avenue wall performance after wall construction and after adding the surcharge. In these two models, soil was represented by Mohr-Coulomb material elements, and geosynthetic reinforcements were represented by cable elements, the built-in structural elements of FLAC. The cable elements were basically elastic material elements with interfaces. The advantages of using cable elements were a simpler model geometry, direct axial stress-strain information, and computational time savings. COMPA and COMPS were the composite property models that simulated the Rainier Avenue wall performance after wall construction and after adding the surcharge. In these models, only anisotropic elastic material elements were used. The GRS composite moduli were obtained by numerically analyzing the UCD test data.

Each model included four parts:

- PART I: Mesh Generation and Foundation Soil: grids and lines were used in this section to form the model mesh of the Rainier Avenue wall. The foundation soil was also created in this section.
- PART II: Input Properties: input soil and geosynthetics properties were defined in this section.
- PART III: Wall Constructions: the body of the Rainier Avenue wall was created with the defined input properties in this section.
- PART IV: Modeling Result Exporting: deflection information and axial forces in the geosynthetics (cable elements) were recorded and exported for further reduction and investigation.

3.2.1 Models 5008 and 5008p2

The FLAC complex models 5008 and 5008p2 consisted of the cable elements, representing the geosynthetic reinforcement, and the Mohr-Coulomb elements, representing the soil. Model 5008 simulated the Rainier Avenue wall performance right after its construction, and Model 5008p2 simulated the wall performance after the surcharge had been applied. The following modeling techniques were used in an effort to accurately model a GRS retaining structure like the Rainier Avenue wall.

1. Mesh generation.
 - 1.1. The unreinforced backfill of the GRS retaining structure models had to be extended a distance at least equal to the length of "reinforced zone" to eliminate boundary effects. For cases in which the unreinforced backfill has an irregular shape or had a length shorter than the "reinforced zone," real boundary conditions had to be modelled.
 - 1.2. The foundation part of the GRS retaining structure models had to be extended at least to a depth equal to one "height of the geosynthetic reinforced wall" to eliminate boundary effects. This technique is relatively important when the settlement of the GRS retaining structure is a major issue.
 - 1.3. For the portion in front of the wall face, as with the unreinforced backfill, the irregular shape and shorter length boundary had to be modeled. Otherwise, the horizontal boundary in front of the wall face had to be extended at least one "length of reinforcement" to eliminate boundary effects.
 - 1.4. Except for the surcharge, the same geometry and mesh generation were used for both models 5008 and 5008p2 so that results could be compared.
2. Unbalanced force, horizontal grid velocity, and vertical grid velocity were monitored during the iteration to ensure that the model reached its equilibrium.

3. Plane strain soil strength properties (friction angles, cohesion, and elastic moduli) were used when the soil retaining structures were modeled. Plane strain strength properties of backfill soil of the Rainier Avenue wall were obtained from the UCD tests.
4. When soil modulus was assigned, the confining pressure effects had to be considered. The lower part of the wall has a higher soil modulus because of the higher confining pressure, and the higher part of the wall has a lower soil modulus because of less confining pressure. This assumption was verified by the soil-only UCD test results.
5. For woven geosynthetics, in-isolation tensile modulus could be used in the models. However, for nonwoven geosynthetics, in-soil confining effect had to be considered when the tensile modulus was selected. Results of UCD test indicated that the tensile moduli of nonwoven geosynthetics increase when the geosynthetics are confined in soil (Boyle, 1995).
6. The 2 percent horizontal strain secant moduli of geosynthetics were measured at the strain rate applied to the reinforcing layers during wall construction and were used in these models to be consistent with the observed wall deformations and geosynthetic strain measurements.
7. The FLAC models were not sensitive to the in-soil thickness of the geosynthetics. However, once the in-soil thickness had been decided, the cross-sectional area, elastic modulus, and perimeter of the cable element had to be calculated with the same in-soil thickness values.
8. Interface properties of the cable elements.
 - 8.1. The interface cohesion (**sbond**)⁴ of the cable elements should be set equal to the soil cohesion.
 - 8.2. The stiffness of woven geosynthetics could be used as the interface stiffness of the cable elements (**kbond**).

⁴ Bold words are the input symbols in FLAC.

- 8.3. The interface friction angle (**sfric**) depends on the relative movements that happen between the soil and the geosynthetic reinforcement. Results of pull-out tests with the same materials can be a good reference. In the Rainier Avenue wall models, the full soil friction angle was used as the interface friction angle for polyester geosynthetics; 2/3 of the soil friction angle was used as the interface friction angle for polypropylene geosynthetics.
- 8.4. The installed, ultimate tensile strengths of geosynthetics were used as the tensile limit (tensile yield strength, **yield**) of geosynthetic reinforcement.
- 8.5. A small value, for example, 10Pa, is suggested as the compression limit (**ycomp**) when cable elements are used to model geosynthetic reinforcement.
9. A subroutine function "batter," edited with FISH⁵, was developed in this project to simplify the procedures for altering the model geometry and inputting the properties. This subroutine can be easily updated to be used in other GRS retaining structure models.
10. After each layer's construction, equilibrium was reached to obtain the best results.
11. Because the inclinometer was installed before the backfill had been placed, the deflection of every construction stage had to be recorded and accumulated to compare with the inclinometer measurements.
12. An EXCEL file was also developed in this project to reduce the data from the FLAC models. It is capable of reducing the raw data obtained from the FLAC model, storing the field instrumentation measurements, and plotting the data reduction results. A manual on how to use this EXCEL file is included in Volume II of this report.

⁵ FISH is the installed coding language of FLAC.

Successful simulation results were obtained from both models 5008 and 5008p2. Figure 5 shows the face deflection results of both models compared with the average survey measurements. Average deflection survey measurements were used to eliminate human errors and the differences between survey measurements. Both models simulated reasonable face deflections and the locations where the maximum deflection was observed. Figure 6 shows the deflection results of both models at 9 ft behind the wall face in comparison to the inclinometer measurements at the same location. The results of both models agreed well with the field measurements. Model 5008 tends to under-estimate deflections in the lower half of the wall, but it over-estimated deflections in the upper half of the wall. However, model 5008p2 tended to under-estimate the deflection throughout the entire wall.

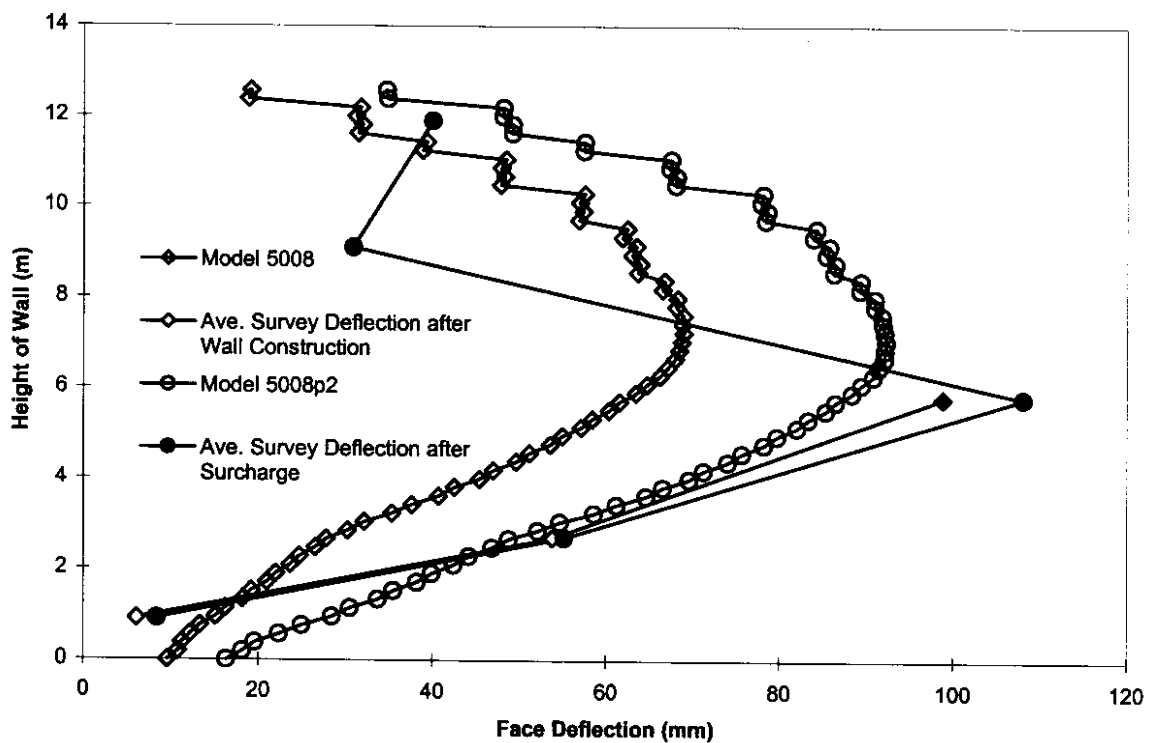


Figure 5. Face Deflection Results of Models 5008 and 5008p2.

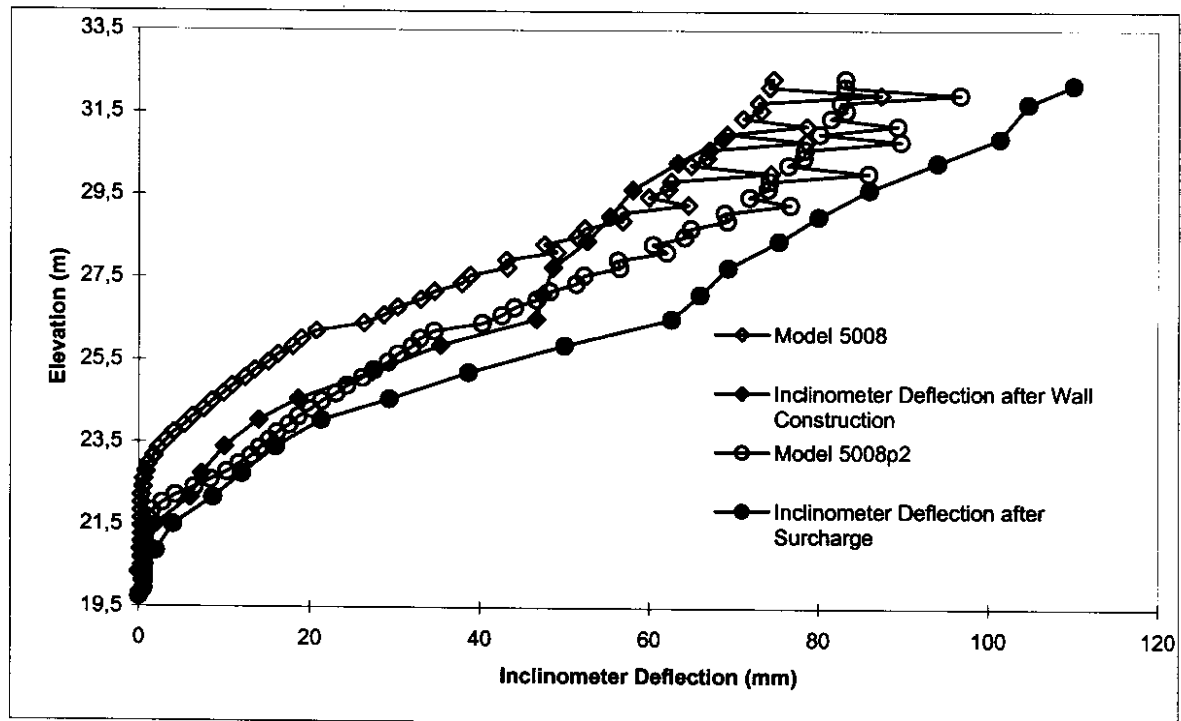


Figure 6. Inclinator Deflection Results of Models 5008 and 5008p2 (inclinator located at 9 ft behind wall face).

Figure 7 shows the strain distribution of the instrumented geosynthetic reinforcement layers of model 5008 in comparison to the strain gage and extensometer measurements. Figure 8 is the same type of plot as Fig. 7 for model 5008p2. As shown in Figs. 7 and 8, results of models 5008 and 5008p2 agreed with the values of maximum strains of the geosynthetic layers and the strain distribution along the geosynthetic reinforcements. Model 5008 showed the maximum strain location of layer 4 closer to the wall face than the instrumentation did; however the difference was less than 30 cm. Model 5008 also tended to over-estimate strains in the higher part of the wall; however, the difference was less than 0.5 percent strain. As shown in Fig. 8, the strain distribution of model 5008p2 showed "second peaks" in higher geosynthetic layers, which indicates that a higher strain plane may be generated as the surcharge is applied.

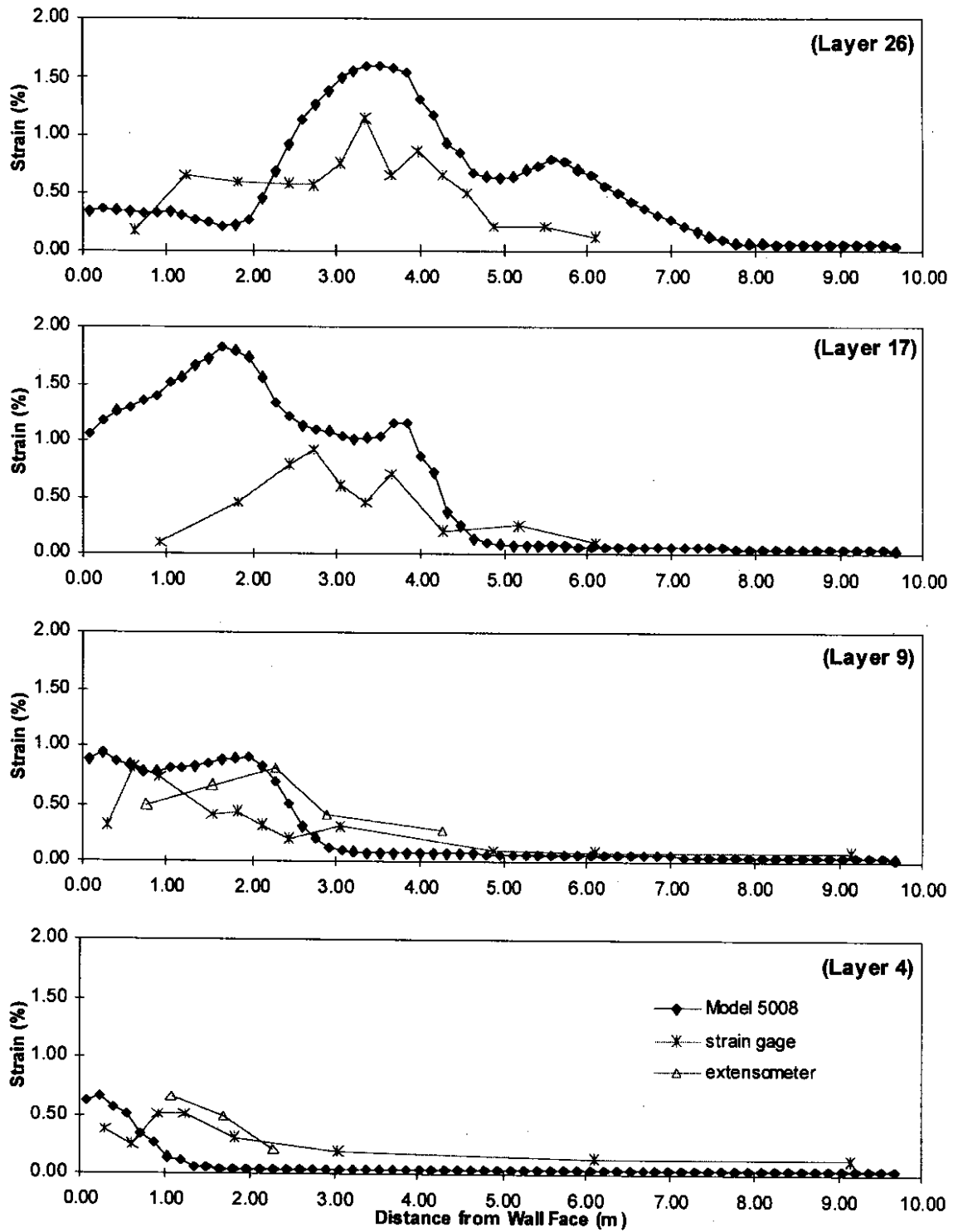


Figure 7. Strain Distribution along the Instrumented Layers, after Wall Construction.

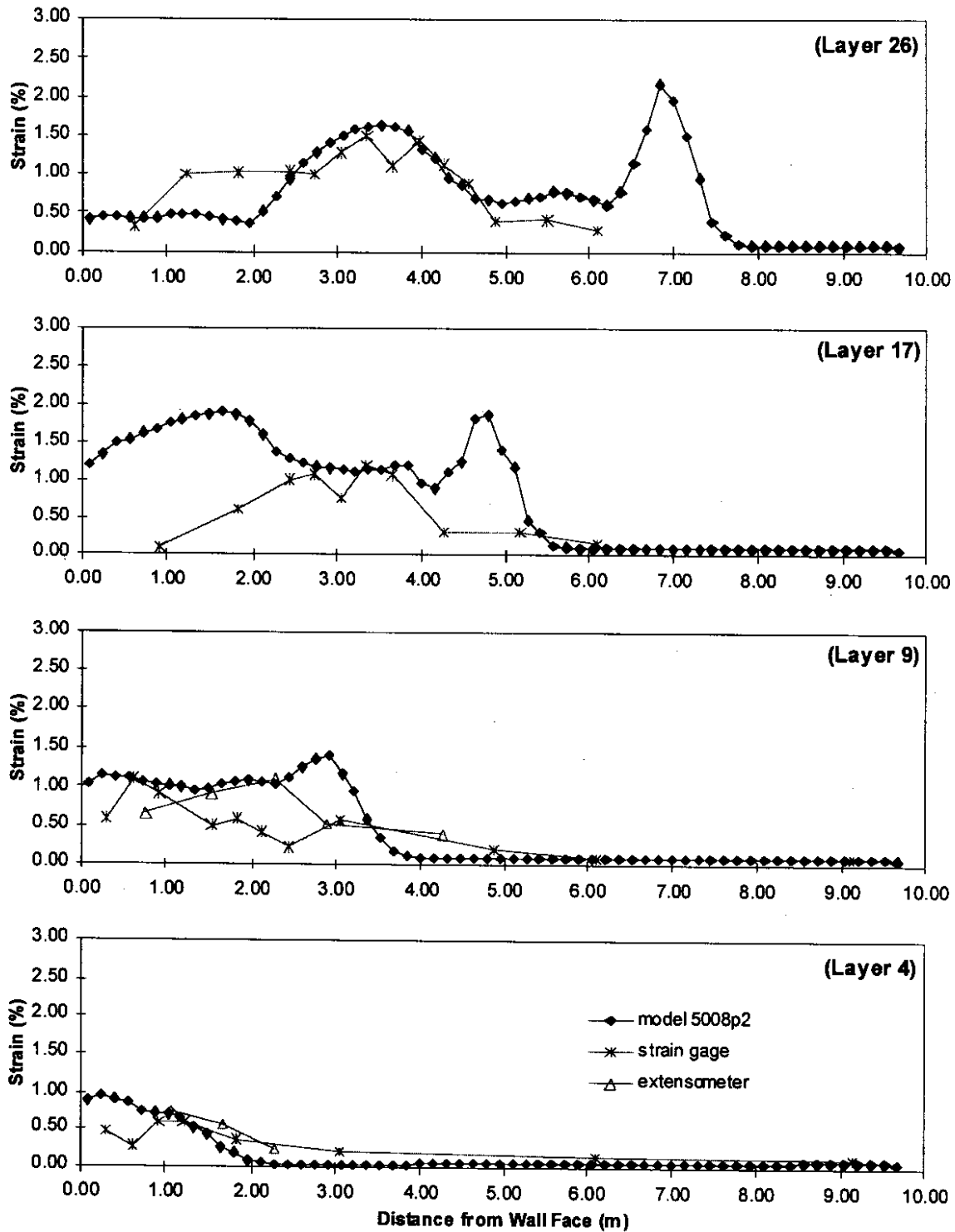


Figure 8. Strain Distribution along the Instrumented Layers, after Surge.

A parametric study was also performed on model 5008 to examine its sensitivity to the input properties. In the parametric study, maximum deflections of the wall model were examined by varying the input properties of the soil and geosynthetics, i.e., the tensile moduli of geosynthetics, the soil friction angle, the soil cohesion, and the soil moduli. Figures 9 to 12 show the results of this study. The maximum deflections increased when the tensile moduli of geosynthetics decreased (Fig. 9). The same tendency was also observed when the soil friction angle changed (Fig. 10). Although the maximum deflections decreased slightly when the soil cohesion was decreased from 8 kPa to 6 kPa (Fig. 11), they increased as the soil cohesion decreased further (Fig. 11). However, the maximum deflections decreased when the soil moduli decreased. Reasons for this phenomenon might involve the external stability and anisotropy of the GRS elements. Generally speaking, the overall deflections of the wall model increased as the input strength properties decreased; and the overall deflections of the wall model decreased as the input strength properties increased. Further parametric studies that examine more input properties and other performance information will be conducted in Phase III research.

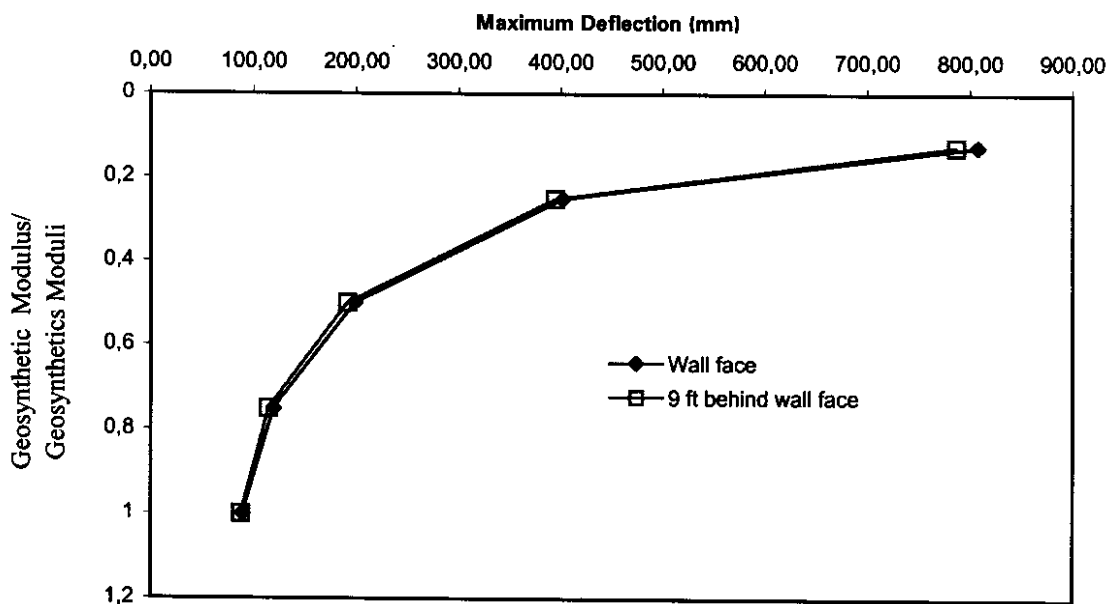


Figure 9. Maximum Deflection vs. Geosynthetic Modulus

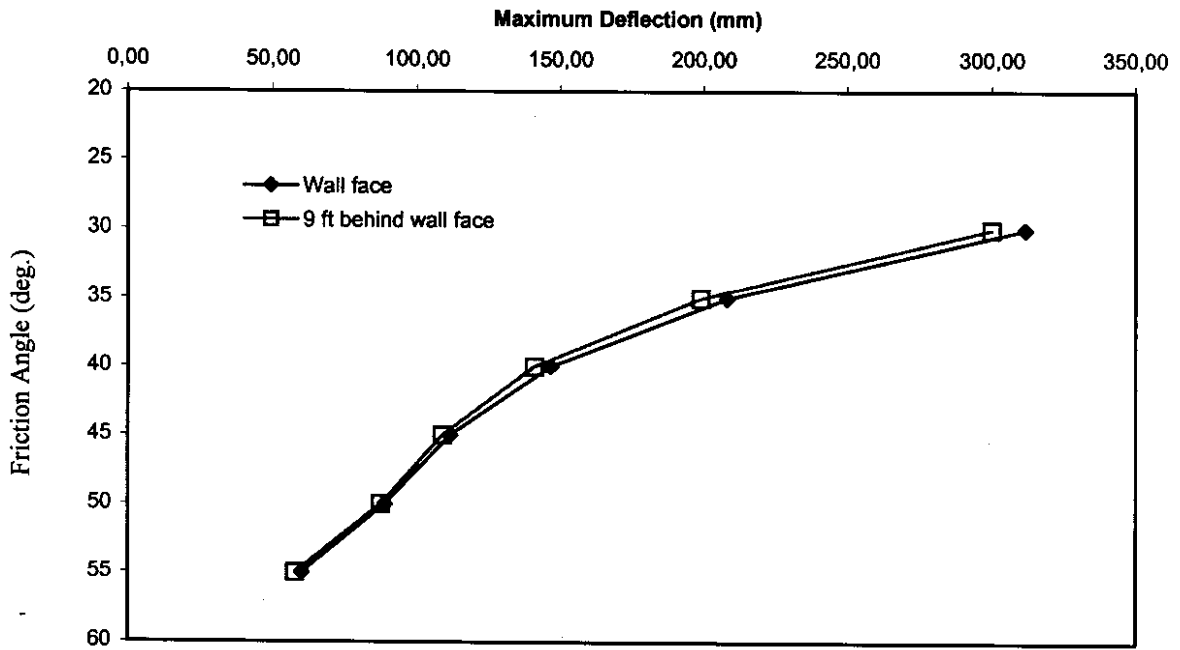


Figure 10. Maximum Deflection vs. Soil Friction Angle

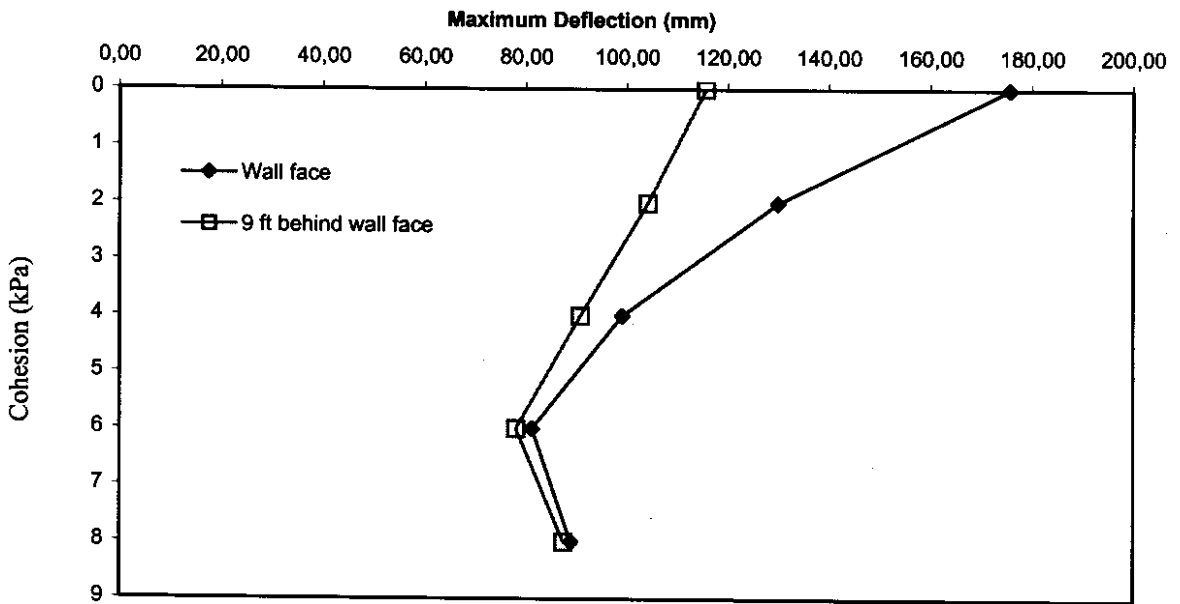


Figure 11. Maximum Deflection vs. Soil Cohesion

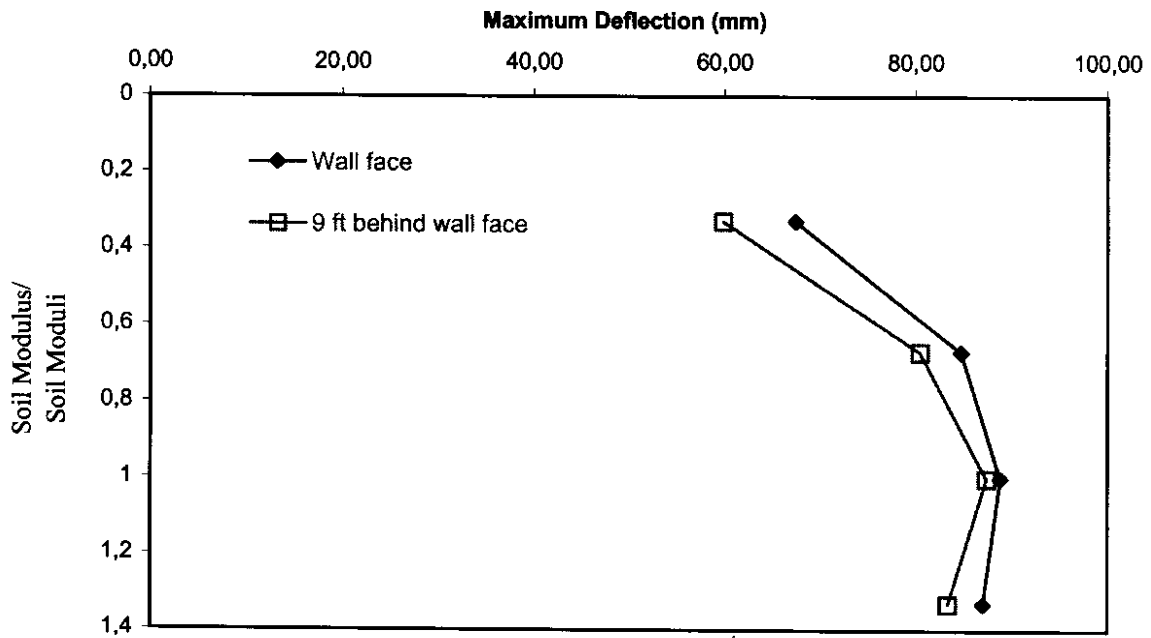


Figure 12. Maximum Deflection vs. Soil Moduli

3.2.2 Models COMPA and COMPS

The FLAC composite property models COMPA and COMPS consisted of only anisotropic elastic material elements. The input strength properties of these anisotropic elastic material elements were the horizontal modulus, the vertical modulus, and the horizontal-vertical plane shear modulus. Model COMPA simulated the Rainier Avenue wall performance after its construction, and model COMPS simulated wall performance after the surcharge had been applied. Both COMPA and COMPS had the same mesh geometries as the complex models 5008 and 5008p2 so that the modeling results could be compared. The modeling techniques used in these two models were as follows:

1. The same mesh generation techniques that were used in models 5008 and 5008p2 were applied to models COMPA and COMPS.
2. Unbalanced force, horizontal grid velocity, and vertical grid velocity were monitored during the iteration to ensure that the model reached its equilibrium.

3. Anisotropic GRS composite moduli (Figs. 3 and 4) obtained by analyzing the UCD test data were used as the input moduli of the reinforced zone in these two models. However, the composite moduli had to be adjusted because the volume ratio of soil to geosynthetic in the Rainier Avenue wall was different from the ratio in the UCD specimen.
4. Anisotropic plane strain soil moduli (Fig. 2) obtained from UCD test data were used as the input moduli of the unreinforced zones in these two models.
5. The GRS composite moduli were described with the effective soil confining pressure (Figs. 3 and 4). Therefore, models COMPA and COMPS had different input properties for the same locations because the effective soil confining pressure distribution in the wall changed after the surcharge was applied.
6. After each layer's construction, equilibrium was reached to obtain the best result.
7. Because the inclinometer was installed before the backfill had been placed, the deflection of every construction stage had to be recorded and accumulated to compare with the inclinometer measurements.
8. An EXCEL file was also developed in this project to reduce the data from the FLAC models. It is capable of reducing the raw data obtained from the FLAC model, storing the field instrumentation measurements, and plotting the data reduction results. The same manual on how to use the EXCEL file for complex models (described in Volume II of this report) can be used for this EXCEL file as well.

Successful simulation results were also obtained from the models COMPA and COMPS. Figure 13 shows the face deflection result of model COMPA in comparison to the results of model 5008 and the averaged survey measurements. Figure 14 shows the deflection result of model COMPA at 9 ft behind the wall face in comparison to the results of model 5008 and the inclinometer measurements at the same location. Figure 15 shows the face deflection results of model COMPS in comparison to the results of model 5008p2 and the averaged survey measurements. Figure 16 shows the deflection result of

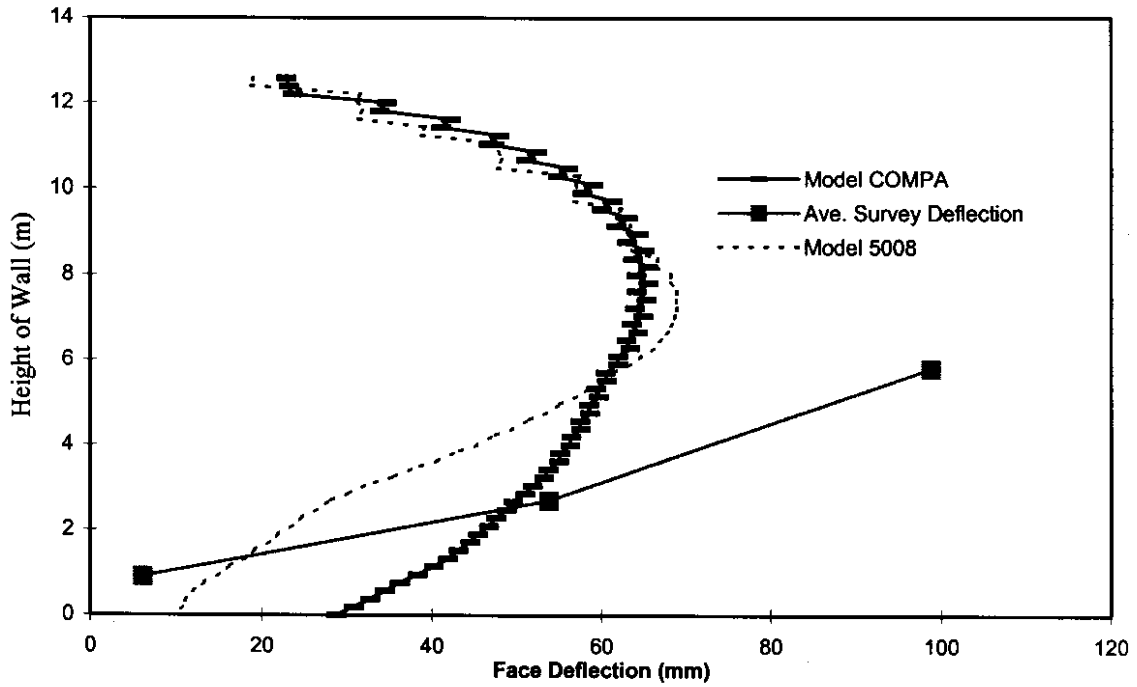


Figure 13. Face Deflection Result of Model COMPA.

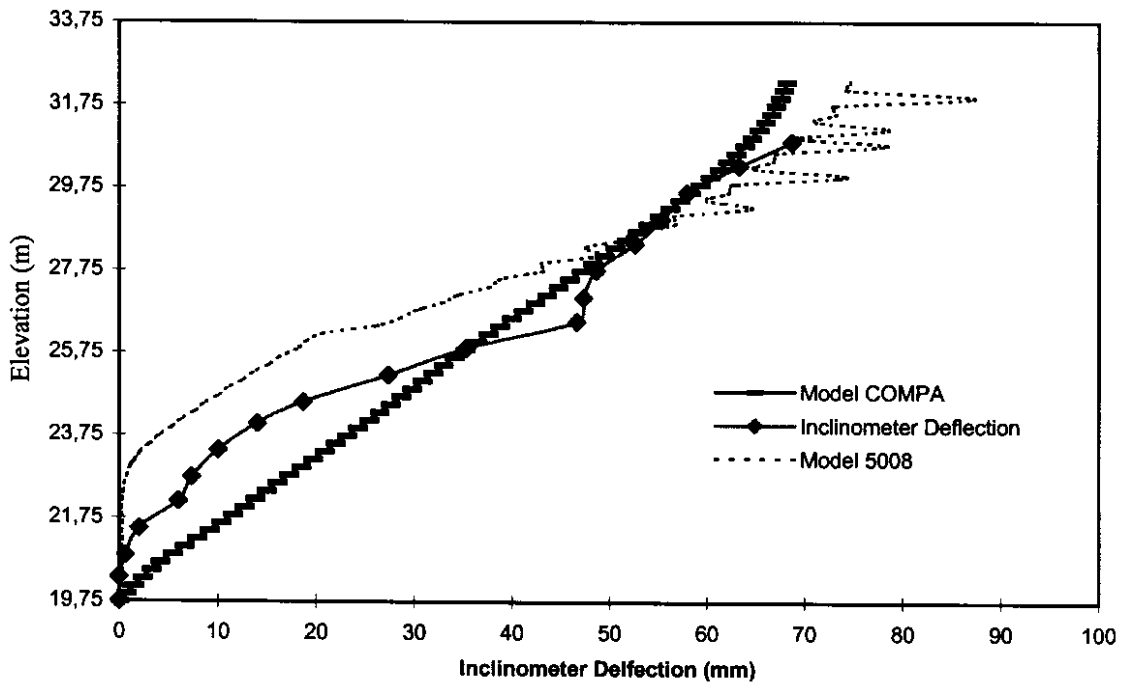


Figure 14. Inclinator Deflection Result of Model COMPA.

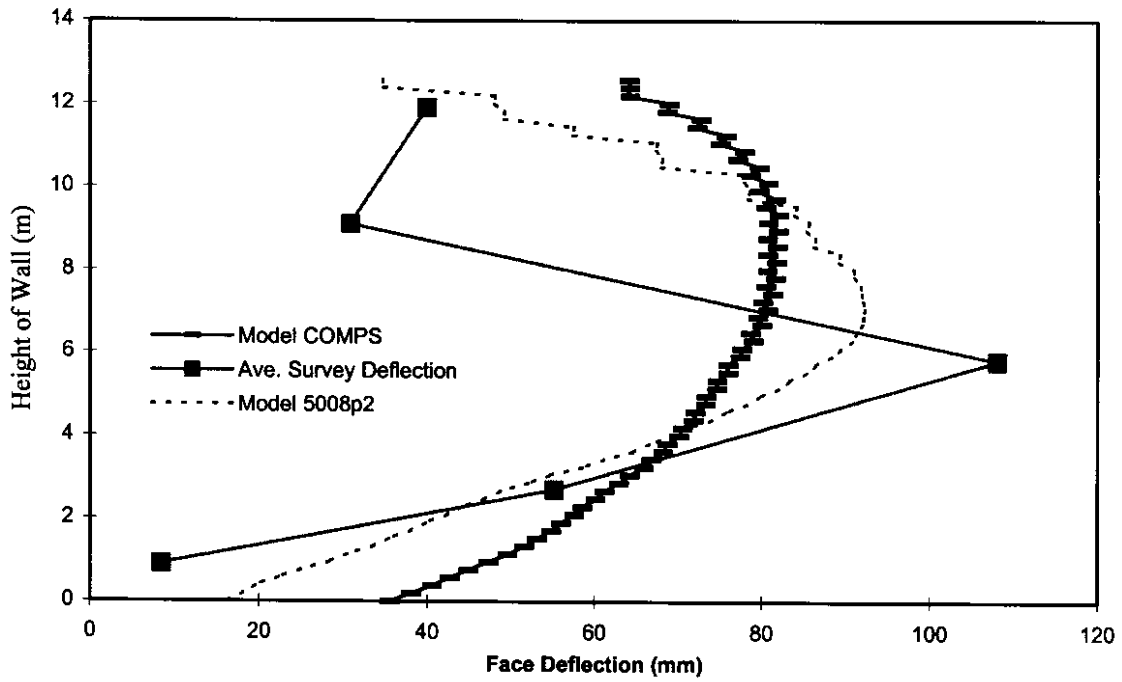


Figure 15. Face Deflection Result of Model COMPS.

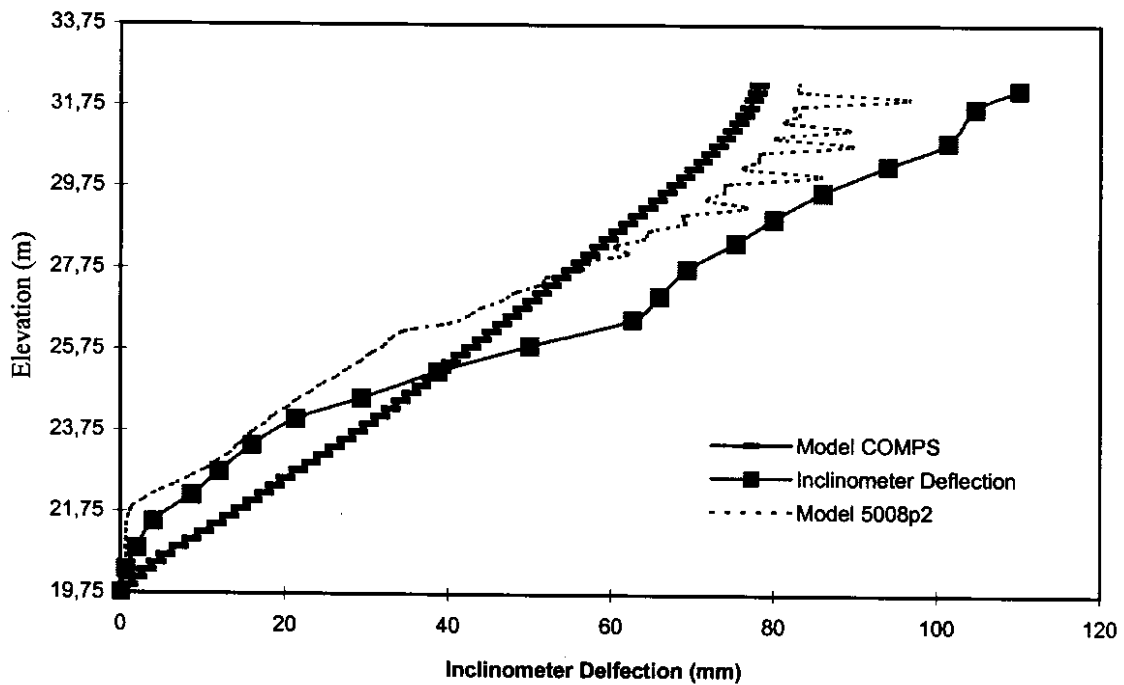


Figure 16. Inclinator Deflection Result of Model COMPS.

model COMPS at 9 ft behind the wall face in comparison to the results of model 5008p2 and the inclinometer measurements at the same location. The results of models COMPA and COMPS agreed with the complex models (models 5008 and 5008p2), as well as the field instrumentation results.

Because the GRS composite moduli were sampled at 1 percent horizontal strain of the UCD GRS specimens, both models tended to overestimate the deflection in the lower half of the wall (the average strain of the lower half of wall was about 0.65 percent after construction and 0.75 percent after the surcharge had been applied). They also underestimated the deflection in the upper half of the wall (the average strain of the lower half of wall was about 1.3 percent after construction and 1.5 percent after the surcharge had been applied).

4. CONCLUSIONS AND SUGGESTIONS

The conclusions and suggestions for further research on GRS retaining structures obtained from this project are as follows:

1. The developed transversely isotropic elasticity model for GRS elements should be applied to more UCD test results. The behaviors of GRS composites sampled at different horizontal strains, for example, 0.5 percent, 1.5 percent, and 2 percent, should be analyzed.
2. If possible, more UCD tests should be performed on more polyester GRS and geogrid GRS to increase our understanding of the behavior of all GRS composites.
3. The use of complex numerical models with structural elements (cable elements) and Mohr-Coulomb material elements (models 5008 and 5008p2) is feasible for modeling the performance and working stress-strain distribution of GRS retaining structures like the Rainier Avenue wall. The same modeling techniques should be applied on more case histories to further examine the capability of this type of model.
4. The results of the complex model change when the input soil cohesion changes. This phenomenon generates uncertainty about the modeling results when the complex model is used to model a GRS wall with sand backfill. In this research, an apparent cohesion of 8 kPa was selected as a reasonable value for the soil backfill on the basis of visual observations and to obtain the best modeling results. Further investigation of the issue is warranted.
5. The advantages of using composite property models are a shorter computation time, the ability to analyze anisotropic working stress-strain distributions in GRS retaining structures, and a sounding theory for selecting input properties.
6. The disadvantage of using composite property models is a lack of direct access to stress-strain information for geosynthetic reinforcements. However, this

disadvantage can be overcome when more GRS composite moduli are sampled at different horizontal strains. The stress-strain distribution of GRS retaining structures can then be analyzed with composite property models, given the input of moduli sampled over a reasonable strain range.

5. REFERENCES

- Allen, T.M., Christopher, B.R., and Holtz, R.D., (1992), "Performance of a 12.6 m high geotextile wall in Seattle, Washington", Geosynthetic-Reinforced Soil Retaining Walls, Int. Symp. on Geosynthetic-Reinforced Soil Retaining Walls. Balkema Publ., pp. 81-100.
- Boyle, S.R., (1995), "Deformation Prediction of Geosynthetic Reinforced Soil Retaining Walls", PhD. Dissertation, University of Washington, Seattle, 391p
- Christopher, B.R., Holtz, R.D., and Allen, T.M. (1990), "Instrumentation for a 12.6 m high geotextile-reinforced wall", Performance of Reinforced Soil Structures, British Geotechnical Society Conference, Glasgow. pp. 73-78.
- Holtz, R.D., Allen, T.M., and Christopher, B.R., (1991), "Displacement of a 12.6 m high geotextile-reinforced wall", Proc. Tenth European Conference on Soil Mechanics and Foundation Engineering, Florence. pp. 725-728.

6. BIBLIOGRAPHY

- Boyle, S.R., and Holtz, R.D., (1994), "Deformation Characteristics of Geosynthetic-Reinforced Soil", 5th International Conference on Geotextiles and Geomembranes and Related Products, Singapore. Vol.1 pp. 361-364.
- Christopher, B.R., and Holtz, R.D. (1985), "Geotextile Engineering Manual", Report No. FHWA-TS-86/203, Federal Highway Administration, Washington, DC, March 1985, 1044p.
- Holtz, R.D., and Kovacs, W.D., (1981), An Introduction to Geotechnical Engineering, Prentice-Hall, Inc., Englewood Cliffs, NJ, 733p
- Itasca Consulting Group, (1993), "Fast Lagrangian Analysis of Continua Version 3.2", Itasca Consulting Group, Inc., Minneapolis, MN, Vol. I, II, III,
- Lee, W. F., (1997), "Numerical Analysis of a Instrumentation of a Geosynthetic-reinforced Wall", Proc. Geosynthetics'97 Conference, Long Beach, CA, Vol. I, pp. 323-336.